

Controlling blooms of *Planktothrix rubescens* by optimized metalimnetic water withdrawal: a modelling study on adaptive reservoir operation

Chenxi Mi (✉ chenxi.mi@ufz.de)

Helmholtz Centre for Environmental Research

David P. Hamilton

Griffith University

Marieke A. Frassl

German Federal Institute of Hydrology

Tom Shatwell

Helmholtz Centre for Environmental Research

Xiangzhen Kong

Chinese Academy of Sciences

Bertram Boehrer

Helmholtz Centre for Environmental Research

Yiping Li

Hohai University

Jan Donner

Fernwasserversorgung Elbaue-Ostharz GmbH

Karsten Rinke

Helmholtz Centre for Environmental Research

Research Article

Keywords: CE-QUAL-W2, *Planktothrix rubescens*, drinking water reservoir, selective withdrawal, light extinction, deep chlorophyll maximum (DCM)

Posted Date: June 22nd, 2022

DOI: <https://doi.org/10.21203/rs.3.rs-1752651/v1>

License:   This work is licensed under a Creative Commons Attribution 4.0 International License.

[Read Full License](#)

Abstract

Background: Aggregations of cyanobacteria in lakes and reservoirs are commonly associated with surface blooms, but may also occur in the metalimnion as subsurface or deep chlorophyll maxima. Metalimnetic cyanobacteria blooms are of great concern when potentially toxic species, such as *Planktothrix rubescens*, are involved. Metalimnetic blooms of *P. rubescens* have apparently increased in frequency and severity in recent years, so there is a strong need to identify reservoir management options to control it. We hypothesized that *P. rubescens* blooms in reservoirs can be suppressed using selective withdrawal to maximize its export from the reservoir. We also expect that altering the light climate can affect the dynamics of this species. We tested our hypothesis in Rappbode Reservoir (the largest drinking water reservoir in Germany) by establishing a series of withdrawal and light scenarios based on a calibrated water quality model (CE-QUAL-W2).

Results: The novel withdrawal strategy, in which water is withdrawn from a certain depth below the surface within the metalimnion instead of at a fixed elevation relative to the dam wall, significantly reduced *P. rubescens* biomass in the reservoir. According to the simulation results, we defined an optimal withdrawal volume to control *P. rubescens* blooms in the reservoir as approximately 10 million m³ (10% of the reservoir volume) during its bloom phase. The results also illustrated that *P. rubescens* growth can be most effectively suppressed if the metalimnetic withdrawal is applied in the early stage of its rapid growth, i.e., before the bloom occurs. Additionally, our study showed that *P. rubescens* biomass gradually decreased with increasing light extinction and nearly disappeared when the extinction coefficient exceeded 0.55 m⁻¹.

Conclusion: Our study indicates the rise in *P. rubescens* biomass can be effectively offset by selective withdrawal strategy and controlling light intensity beneath the water surface. Considering the widespread occurrence of *P. rubescens* in stratified lakes and reservoirs worldwide, we believe the results will be helpful for scientists and water managers working on other water bodies to minimize the negative impacts of this harmful algae.

1. Introduction And Background

Cyanobacteria can form dense and toxic blooms in lentic waters, which severely threatens the development of aquatic ecosystems and human health (Huisman et al., 2018). Cyanobacteria blooms can block sunlight and their breakdown consumes oxygen that other organisms need to live (Mishra et al., 2019). Additionally, during the growth period, the algae often produce cyanotoxins, which are dangerous for water safety to humans, aquatic organisms and farmed animal stocks without remedies to counteract the effects (Rastogi et al., 2015). A global survey indicates that the cyanobacteria blooms are nowadays increasing in magnitude, frequency and duration in freshwater lakes worldwide (Gallina et al., 2017; Huang et al., 2020; Ho et al., 2019). These blooms are often directly visible because they occur at the surface layer and even form scums allowing management authorities to initiate precautionary measures (Chorus et al., 2000). A different situation arises for subsurface or deep chlorophyll maxima

which may also include dense cyanobacteria populations. They are generally less visible and overlooked (Walsby and Jüttner, 2006) though they can be toxic as well and often occur in sensitive water bodies like drinking water reservoirs. Phytoplankton in subsurface chlorophyll maxima tradeoff between increasingly limited light supply with depth and access to nutrients from deeper layers (Abbott et al., 1984; Cullen, 2015). The light penetrating below the mixed layer is critical for the presence and depth of subsurface chlorophyll layers. Hence the occurrence of subsurface chlorophyll maxima is usually restricted to relatively clear oligo- or mesotrophic lakes and reservoirs (Hamilton et al., 2010; Leach et al., 2018).

Planktothrix rubescens (hereafter *P. rubescens*) is a cyanobacterium that often forms metalimnetic chlorophyll maxima and affects deep oligotrophic waterbodies, including reservoirs and lakes commonly used for drinking water supply (D'Alelio et al., 2011). It is a filamentous cyanobacterium that potentially contains hepatotoxic peptides known as microcystins (Kurmayer and Gumpenberger, 2006; Ernst et al., 2009), so its occurrence in drinking water bodies poses a serious human health concern (Bogialli et al., 2013). *P. rubescens* typically grows in a subsurface layer below the epilimnion of stratified waters (Padisák et al., 2009; Gallina et al., 2017). Its name derives from the characteristic red colour associated with the pigment phycoerythrin, which enhances photon capture of green-shifted light in deeper water layers (Reynolds, 2006).

P. rubescens is highly competitive in nutrient-depleted environments (Carraro et al., 2012) and the subsurface light climate is considered to be critical to its growth (Posch et al., 2012). It regulates the vertical position in water column by adjusting its density according to ambient light levels (Trbojević et al., 2019) in order to generate buoyancy under low light levels. At higher light levels, by contrast, it accumulates carbohydrates which act as a ballast and reduces buoyancy (Walsby and Schanz, 2002). Laboratory experiments and field studies have shown that the depth of neutral buoyancy lies in a range of photosynthetically active radiation (PAR) between $0.28 \text{ mol m}^{-2} \text{ d}^{-1}$ and $0.51 \text{ mol m}^{-2} \text{ d}^{-1}$ (Walsby et al., 1983; Walsby et al., 2004). After initially being dispersed in the well-mixed water column in spring, *P. rubescens* develops subsurface 'blooms' as stratification strengthens in summer, if the depth of neutral buoyancy is greater than the mixed layer depth (Lürling et al., 2020). Decreasing ambient light in autumn, followed by deepening of the mixed layer, often causes the subsurface population to be dispersed into the surface mixed layer again, and has occasionally been associated with surface blooms (Fee, 1976; Walsby and Jüttner, 2006).

Previous research has confirmed that increased duration and strength of seasonal stratification, due to projected climate changes (Shatwell et al., 2019), could favor the dominance of buoyancy-regulating *P. rubescens* (Carraro et al., 2012; Knapp et al., 2021), and therefore finding an effective strategy to control its growth receives increasing concern. Despite a series of physical, chemical and biological strategies (including dredging, physical flushing, application of precipitating phosphorus, selective grazing, etc.) in mitigating cyanobacterial blooms (Paerl, 2018), most of them merely dealt with the surface type typical for eutrophic/hypertrophic lakes (Gu et al., 2021; Rigosi and Rueda, 2012; Lewis Jr et al., 2011) but neglected subsurface blooms typical for mesotrophic lakes (e.g. metalimnetic blooms of *P. rubescens*).

In reservoir management, selective withdrawal – i.e. removing water from a specific outlet height – is an interesting option. It has been used to affect biogeochemical cycling (Weber et al., 2017) or to control vertical heat exchange (Mi et al., 2020b). Previous studies have illustrated that selective withdrawal can redistribute the dissolved oxygen in the water column (Carr et al., 2019), decrease nutrient concentrations (Dehbalaei and Javan, 2018), and change the dominant algal assemblages (Rigosi and Rueda, 2012). This body of research indicates that selective water withdrawal may also have potential to control *P. rubescens* blooms but this has never been explored so far. For concrete management targets, detailed recommendations for optimal withdrawal timing, discharge and duration need to be identified. Our research aims at bridging this research gap by a systematic analysis of alternative withdrawal strategies with respect to their effects on *P. rubescens* dynamics.

Besides management measures also the surrounding environmental factors come into play and light availability appears to be a key factor for *P. rubescens* growth (e.g. Gallina et al., 2017; Walsby and Jüttner, 2006). Recent observations of rising colored dissolved organic matter (Zhou et al., 2018), as well as any changes in phytoplankton biomass (Williams et al., 2018) and non-algal particles (Abdelrhman, 2016), may modify light extinction in lentic waters, and are therefore likely to affect *P. rubescens* populations. Accordingly in our study, we also included an analysis checking the response of *P. rubescens* dynamics to different light extinction conditions.

In this study, the two-dimensional (2D) water quality model (CE-QUAL-W2, hereafter W2) was used to simulate the dynamics of *P. rubescens* in Germany's largest drinking water reservoir, Rappbode Reservoir. Our previous research has confirmed the dominance of *P. rubescens* in the metalimnion of the reservoir in summer (Wentzky et al., 2019), and the calibrated W2 showed good performance in capturing the spatial and temporal distribution of *P. rubescens* as well as nutrient and oxygen dynamics in the water column (Mi et al., 2020a). In the current study, several application-oriented scenarios were designed based on the established model, with the aim to address three questions:

- (1) Is it possible to influence or control the population of *P. rubescens* by selective water withdrawal?
- (2) What is the optimal timing and amount of water for the withdrawal strategy to remove *P. rubescens*?
- (3) How does light extinction within the water column affect the population and growth period of *P. rubescens*?

Since the occurrence of *P. rubescens* is a common and increasing problem in stratified lakes and reservoirs worldwide (Wentzky et al., 2019; Posch et al., 2012; Knapp et al., 2021), we believe that the importance of this study reaches beyond the case of Rappbode Reservoir, and it provides a strategy that could be considered by scientists, stakeholders and managers working on other reservoirs, which are similarly affected by subsurface blooms of *P. rubescens*.

2. Methods

2.1 Study site

Rappbode Reservoir (51.74 °N, 10.89 °E) is located in the Harz Mountains in central Germany (crest elevation at 423.6 metres above sea level (masl), Fig. 1). With a maximum water storage of over 100 million m³, Rappbode Reservoir is the largest drinking water reservoir in the country, providing drinking water for over one million people. The reservoir has a maximum surface area of 395.3 ha, and a maximum depth of 89.0 m (28.6 m mean depth) at full storage. It is fed by the tributaries from Hassel and Rappbode pre-reservoirs, and receives water transfers from the Koenigshuette pre-reservoir (Kong et al., 2021). The reservoir dam has five outlets at different elevations (from 360 to 400 masl in 10 m intervals for drinking water supply) from which the lowest one (at 360 masl) was used for most of the time, and a deep hypolimnetic outlet discharging water into the downstream Wendefurth Reservoir from 345 masl (Mi et al., 2019). The water residence time of the reservoir is approximately one year (344–380 days, Rinke et al., 2013). Rappbode Reservoir is a dimictic waterbody, which stratifies in summer, partly freezes in winter and fully mixes in spring and autumn (Wentzky et al., 2018). The reservoir ecosystem is currently in an meso/oligotrophic state (TP concentration dropped to 0.027 mg L⁻¹ after 1990, see Wentzky et al., 2018). However, recent studies showed that the waterbody experiences regular metalimnetic oxygen minima which is presumably caused by both pelagic (biological activities of *P. rubescens* in the metalimnion) and benthic (sediment oxygen demand) processes (Wentzky et al., 2019; Mi et al., 2020b).

2.2 Water quality model

In this study a two-dimensional water quality model CE-QUAL-W2 (hereafter W2), version 4.1, was used to simulate the Rappbode Reservoir. W2 was launched in 1975 by Edinger and Buchak from the U.S. Army Corps of Engineers. It has been widely used in analyzing thermal structure and eutrophication processes for lakes and reservoirs worldwide (e.g. Jin et al., 2019; Carr et al., 2019; Park et al., 2018; Kobler et al., 2018), and its source code is freely available from the official website (<https://www.cee.pdx.edu/w2/>). As a vertically resolved 2D model, W2 is well suited for simulating waterbodies with a long and narrow shape, which is the case for the Rappbode Reservoir (Rinke et al., 2013).

The model setup was drawn from our previous research in Rappbode Reservoir (see Mi et al., 2020a) on metalimnetic oxygen dynamics and the physical and ecological sub-models were rigorously validated by comparisons with observed data. The reservoir basin is divided into four branches with 106 horizontal segments and 3976 grid cells, and the vertical spacing for each cell is 1 m. According to the dominating phytoplankton community structure, two algae groups (*P. rubescens* and a group representative of other phytoplankton, with physiological parameters linked to diatoms) are differentiated. Besides these, nutrients (nitrogen, phosphorus, silicate), detritus components, dissolved oxygen and water temperature were included in the simulation as state variables. From model output of dry weight of *P. rubescens*, we used a fixed yield ratio to calculate chlorophyll *a* concentration of the algae which is 0.18 mg dry weight/ug chlorophyll *a* (Mi et al., 2020a; Carraro et al., 2012). The base simulation (set as reference, i.e. Scenario R) reproduced observed ecosystem dynamics in Rappbode reservoir with comparatively high accuracy.

As a quantitative description, the validated model showed good performance in capturing water temperature (RMSE = 0.45°C, $R^2 = 0.99$), dissolved oxygen (RMSE = 0.95, $R^2 = 0.84$) and the growth of *P. rubescens* (RMSE = 0.65, $R^2 = 0.56$) in the reservoir (Fig. 2). Additionally, the model satisfactorily reproduced the seasonal distribution of two algae groups (i.e. spring bloom of diatoms and summer bloom of *P. rubescens*) and the phenomenon of metalimnetic oxygen minimum in late summer. For calibration and the detailed validation procedure, as well as the model performance in reproducing other water quality variables in the reservoir, the reader is referred to Mi et al. (2020a). We also performed the sensitivity analysis by changing each input parameter by ($\pm 5\%$ and $\pm 10\%$), and calculated the specific sensitivity coefficients (SSC, Table S1) for the the maximum concentration of *P. rubescens* (see supplement material). Despite changes of the maximum concentration under perturbations of parameters, the model always showed a stable reproduction for the key pattern of *P. rubescens* to be growing in the metalimnion during summer, which indicates model robustness (see Fig S1).

2.3 Scenarios

Scenario V: Effect of metalimnetic withdrawal volume on the *P. rubescens* bloom

We established seven scenarios, with different withdrawal volumes (V) to examine the effectiveness of selective water withdrawal on controlling the *P. rubescens* bloom in Rappbode Reservoir (see Table 1). In 2016, *P. rubescens* concentration (given as chlorophyll *a*) increased rapidly at around 11 m depth (i.e., metalimnion) from day 133 to 248 (see Fig. 2). Accordingly, in the V scenarios, we simulated the selective withdrawal during this period at a constant water depth of 11 m. Selective withdrawal water was directed as discharge towards Wendefurth reservoir (i.e. downstream release) while the withdrawal for drinking water was still taken in all scenarios from the hypolimnion. This deep raw water extraction is the standard case and preferred mode due to low temperature and turbidity in the location.

Table 1

Overview of factors altered for scenarios R, L, V, and T; all other model settings remained identical across all scenarios. Detailed information of each scenario can be referred to the corresponding paragraph in section 2.3. ⁽¹⁾ Metalimnetic withdrawal discharge in scenario V_{\max} is the maximum discharge for each day of the year from 133 to 248, based on long-term measurements (year 1996–2015). ⁽²⁾ Metalimnetic withdrawal discharge in scenario T is the maximum discharge at each day from 182 to 205, based on long-term measurements.

	Scenario	Light extinction coefficient (m^{-1})	Metalimnetic withdrawal depth	Metalimnetic withdrawal discharge	Metalimnetic withdrawal timing
	Scenario R	0.45	–	–	–
	Scenario $L_{0.35}$	0.35	–	–	–
	Scenario $L_{0.55}$	0.55	–	–	–
	Scenario $L_{0.65}$	0.65	–	–	–
	Scenario $L_{0.90}$	0.9	–	–	–
	Scenario V_{\min}	0.45	11 m below surface	Measurements in 2016	Day 133 to 248
	Scenario V_1	0.45	11 m below surface	$1 \text{ m}^3 \text{ s}^{-1}$	Day 133 to 248
	Scenario V_2	0.45	11 m below surface	$2 \text{ m}^3 \text{ s}^{-1}$	Day 133 to 248
	Scenario V_3	0.45	11 m below surface	$3 \text{ m}^3 \text{ s}^{-1}$	Day 133 to 248
	Scenario V_4	0.45	11 m below surface	$4 \text{ m}^3 \text{ s}^{-1}$	Day 133 to 248
	Scenario V_5	0.45	11 m below surface	$5 \text{ m}^3 \text{ s}^{-1}$	Day 133 to 248
	Scenario V_{\max}	0.45	11 m below surface	Maximum in historical measurements ⁽¹⁾	Day 133 to 248
T_{early}	Scenario T_{133}	0.45	11 m below surface	Maximum in historical measurements ⁽²⁾	Day 133 to 156

	Scenario	Light extinction coefficient (m⁻¹)	Metalimnetic withdrawal depth	Metalimnetic withdrawal discharge	Metalimnetic withdrawal timing
	Scenario T ₁₄₀	0.45	11 m below surface	Maximum in historical measurements ⁽²⁾	Day 140 to 163
	Scenario T ₁₄₇	0.45	11 m below surface	Maximum in historical measurements ⁽²⁾	Day 147 to 170
	Scenario T ₁₅₄	0.45	11 m below surface	Maximum in historical measurements ⁽²⁾	Day 154 to 177
	Scenario T ₁₆₁	0.45	11 m below surface	Maximum in historical measurements ⁽²⁾	Day 161 to 184
T _{bloom}	Scenario T ₁₆₈	0.45	11 m below surface	Maximum in historical measurements ⁽²⁾	Day 168 to 191
	Scenario T ₁₇₅	0.45	11 m below surface	Maximum in historical measurements ⁽²⁾	Day 175 to 198
	Scenario T ₁₈₂	0.45	11 m below surface	Maximum in historical measurements ⁽²⁾	Day 182 to 205
	Scenario T ₁₈₉	0.45	11 m below surface	Maximum in historical measurements ⁽²⁾	Day 189 to 212
	Scenario T ₁₉₆	0.45	11 m below surface	Maximum in historical measurements ⁽²⁾	Day 196 to 219
T _{late}	Scenario T ₂₀₃	0.45	11 m below surface	Maximum in historical measurements ⁽²⁾	Day 203 to 226
	Scenario T ₂₁₀	0.45	11 m below surface	Maximum in historical measurements ⁽²⁾	Day 210 to 233
	Scenario T ₂₁₇	0.45	11 m below surface	Maximum in historical measurements ⁽²⁾	Day 217 to 240

Scenario	Light extinction coefficient (m^{-1})	Metalimnetic withdrawal depth	Metalimnetic withdrawal discharge	Metalimnetic withdrawal timing
Scenario T ₂₂₄	0.45	11 m below surface	Maximum in historical measurements ⁽²⁾	Day 224 to 247
Scenario T ₂₃₁	0.45	11 m below surface	Maximum in historical measurements ⁽²⁾	Day 231 to 254

In scenario V_{\min} , metalimnetic water was withdrawn with the same (downstream) discharge as originally measured during the corresponding period in 2016. Considering the relatively low discharge in this scenario (average $0.66 \text{ m}^3 \text{ s}^{-1}$), we designed another scenario with the maximum metalimnetic withdrawal discharge. This was defined by using the daily maximum discharge from historical measurements, at each specific day, from day 133 to 248 between 1996 and 2015 (scenario V_{\max}). In this scenario, the average discharge during the period is $5.43 \text{ m}^3 \text{ s}^{-1}$, i.e. nearly eight times larger than in V_{\min} . To analyze the effect of withdrawal volume on *P. rubescens* in a systematic way, we finally developed five scenarios in which the discharge was increased from $1 \text{ m}^3 \text{ s}^{-1}$ to $5 \text{ m}^3 \text{ s}^{-1}$ at intervals of $1 \text{ m}^3 \text{ s}^{-1}$, during the period mentioned above (day 133 to 248, scenarios V_1 - V_5). We analyzed the results by segmented regression, using the R package “segmented” (Muggeo and Muggeo, 2017), in order to elucidate the relationship between metalimnetic withdrawal volume and the maximum *P. rubescens* concentration.

Scenario T: Effect of metalimnetic withdrawal timing on the *P. rubescens* bloom

To characterize the time window (T) of selective water withdrawal that most effectively controls *P. rubescens*, we developed 15 sub-scenarios in Scenario T in which metalimnetic withdrawal was applied over a duration of 23 days. We varied the starting time of each period from day 133 to 231 at one-week intervals (i.e., T₁₃₃, T₁₄₀,... T₂₃₁). We used the maximum daily discharge at each day between day 182 to 205 (year 1996–2015), which represents the midmost of the applied timespans, for defining the withdrawal amounts (Table 1). This ended up in an average discharge of $4.39 \text{ m}^3 \text{ s}^{-1}$ in all T-scenarios, representing 8.7 million m^3 and accounts for 9% of the reservoir storage. For making these results tangible and easier to present, we divided them into three main groups with the first five scenarios as the early group phase (T_{early}), the second group of five as the main bloom phase (T_{bloom}), and the third group as the late bloom phase of decreasing biomass (T_{late}, see also Table 1). At all other times the discharge and withdrawal elevation for the downstream reservoir and the drinking water supply were the same as in the reference simulation (i.e., Scenario R).

Scenario L: Effect of the background light condition on *P. rubescens* growth

In this scenario, we varied the light environment (L) experienced by *P. rubescens*. Photosynthetically active radiation (PAR) at depth z (I_z in $\text{mol m}^{-2} \text{day}^{-1}$) was calculated according to the Lambert-Beer law:

$$I_z = (1 - \beta) c I_0 e^{-\sum_{i=1}^{i_{max}} \epsilon_i dz_i}$$

1

where I_0 is the downwelling shortwave radiation at the water surface, c is the fraction of shortwave radiation that is PAR, set as 0.5 based on Kirk (1994), β is albedo, set to 0.1 based on Williams (1981), dz_i is the thickness of layer i (always 1 m) and i_{max} is the layer number at depth z , ϵ_i is the light extinction coefficient at layer i , which consists of the extinction in algal-free water (ϵ_b) plus light extinction from phytoplankton (specific extinction coefficient for diatoms, ϵ_{diatom} and *P. rubescens*, $\epsilon_{P. rubescens}$):

$$\epsilon_i = \epsilon_b + \epsilon_{diatom} A_{diatom} + \epsilon_{P. rubescens} A_{P. rubescens}$$

2

Since the concentration of diatoms, A_{diatom} and *P. rubescens*, $A_{P. rubescens}$ varies between layers, light extinction is layer-specific.

To illustrate the response of *P. rubescens* to light conditions, we compared results in the reference simulation (i.e., a background light extinction coefficient ϵ_b of 0.45 m^{-1} , scenario R) with scenarios where ϵ_b was either decreased to 0.35 m^{-1} , or increased to 0.55 m^{-1} , 0.65 m^{-1} and 0.9 m^{-1} (scenario $L_{0.35}$, $L_{0.55}$, $L_{0.65}$, $L_{0.90}$, respectively) which represents the realistic range of the extinction in Rappbode Reservoir (see Fig S4 in Mi et al. (2020a)).

3. Results

3.1. Scenario V: Effect of metalimnetic withdrawal volume on the *P. rubescens* bloom

Metalimnetic water withdrawal effectively decreased the *P. rubescens* bloom in Rappbode Reservoir. Although the seasonal distribution of *P. rubescens* in the V-scenarios remained similar to that in the reference simulation, its biomass concentrations gradually decreased in scenarios with increasing metalimnetic discharge (Fig. 3, 4). In the reference simulation (i.e., no metalimnetic withdrawal), the average and maximum concentration of *P. rubescens* (all expressed as chlorophyll *a*) in the metalimnion during summer (10 to 12 m depth, day 180 to 240) were 4.0 and $6.12 \mu\text{g L}^{-1}$ respectively. These values decreased, for example, to 3.5 and $5.5 \mu\text{g L}^{-1}$ under scenario V_{min} (metalimnetic withdrawal volume of 6.6 million m^3) and further to 1.1 and $1.9 \mu\text{g L}^{-1}$ under scenario V_{max} (with metalimnetic withdrawal volume of 55.4 million m^3 ; see Fig. 4). This higher metalimnetic discharge was traded off against

decreased water level in the reservoir at the end of the year, from 410 masl under the reference simulation down to 382 masl under scenario V_{\max} (Fig. 3). In other words, the costs of removing *P. rubescens* out of the metalimnion arise in terms of water loss.

The relative effect of increasing metalimnetic withdrawal volume on *P. rubescens* was greatest between scenario V_{\min} and V_1 , while the effect gradually weakened with higher withdrawal volumes (Fig. 4). The results from segmented regression, for withdrawal volume vs *P. rubescens* concentration, indicated a breakpoint at a withdrawal volume of 12.3 million m^3 (i.e., slightly higher than the value under scenario V_1), corresponding to discharge of $1.24 \text{ m}^3 \text{ s}^{-1}$ during the growth period. Below this value the maximum *P. rubescens* concentration decreased at $0.25 \mu\text{g L}^{-1}$ per million m^3 , while above this value the rate of change was only $0.03 \mu\text{g L}^{-1}$ decrease per million m^3 , i.e., one order of magnitude lower. Since under scenario V_1 the maximum concentration of *P. rubescens* (i.e., $3.3 \mu\text{g L}^{-1}$) already decreased to nearly half of that under the reference simulation (i.e., $6.1 \mu\text{g L}^{-1}$) with relatively small change in water withdrawal volume (see Fig. 3), we identified the optimal withdrawal volume to control *P. rubescens* as approximately 10 million m^3 (10% of the reservoir volume), corresponding to discharge of $1 \text{ m}^3 \text{ s}^{-1}$ during the growth period (day 133–248). Based on the results from this optimized scenario, the lowest water level never falls below 408.9 m. This relatively small additional water loss implies that the optimized management only marginally interferes with drinking water security and is therefore widely acceptable by reservoir operators (Fig. 3). Under conditions of extreme drought (e.g. in the year 2003), however, the additional water withdrawal may become a concern.

3.2. Scenario T: Effect of metalimnetic withdrawal timing on the *P. rubescens* bloom

The main growth phase of *P. rubescens* occurs before it attains the maximum abundance. For the reference simulation, the steady increase of *P. rubescens* began around day 130 and ended on day 215 (Fig. 3) when the biomass peaked (scenario R, Fig. 3). The average specific growth rate in the simulation during this period was 0.032 d^{-1} (10 to 12 m depth), and the maximum was 0.098 d^{-1} on day 177. Thus, to compensate for the growth of *P. rubescens*, an average withdrawal rate equivalent to 0.032 d^{-1} would be required from the metalimnetic water layers. In scenario R, i.e., under the actual reservoir operation conditions that largely follow the snowmelt-dominated hydrology of the catchment, the downstream withdrawal was high only early in the year and relatively low afterwards. If this downstream withdrawal was taken entirely from the metalimnion, specific clearance rates could reach up to 0.1 d^{-1} and, for example, reach an average value of 0.052 d^{-1} between day 40 and 90. But this time window is too early and just before *P. rubescens* can start growing (Fig. S2). After this period, i.e., during the phase of positive growth after day 130, water withdrawal decreased with the rates dropped to below 0.01 d^{-1} (Fig. S2). Accordingly, effective removal of the algae can be realized, if the selective withdrawal for the downstream river is timed later in order to have more overlap with the occurrence of *P. rubescens*.

The results from scenario T indicate that the population of *P. rubescens* was most effectively suppressed, if the metalimnetic withdrawal was applied at an early growth stage (i.e., scenarios T_{early}, see Fig. 5, 6). Under these scenarios, the average (maximum) *P. rubescens* concentration at depths from 10 to 12 m always remained below 3.0 µg L⁻¹ (4.0 µg L⁻¹), while the value gradually increased to between 3.0 and 3.3 µg L⁻¹ (4.3 and 5.3 µg L⁻¹) and further above 3.4 µg L⁻¹ (5.5 µg L⁻¹) when water was withdrawn in the blooming (scenarios T_{bloom}) and late bloom stages (scenarios T_{late}). Aside from the standing stock of *P. rubescens*, the timing of its maximum concentration as well as the spatial patterns were not markedly changed in different T scenarios (Fig. 6).

3.3. Scenario L: Effect of the background light condition on *P. rubescens* growth

Growth of *P. rubescens* was gradually suppressed with increased light extinction (Fig. 7). In the reference scenario (background light extinction coefficient $\epsilon_b = 0.45 \text{ m}^{-1}$), the maximum concentration in the metalimnion was 5.4 µg L⁻¹. It increased to 6.7 µg L⁻¹ under scenario L_{0.35} ($\epsilon_b = 0.35 \text{ m}^{-1}$), but decreased to 2.2, 1.3 and 0.5 µg L⁻¹ under scenarios L_{0.55}, L_{0.65}, and L_{0.90}. Additionally, *P. rubescens* reached maximum concentration later in the year under the lower light extinction. In the reference simulation, the concentration peaked at day 215. This peak was advanced to day 185 under the three scenarios with higher light extinction (Fig. 7) but delayed to day 253 under scenario L_{0.35} with lower light extinction. The later development of the elevated concentrations appeared to be related to longer persistence of diatoms in the metalimnion, with a shift from diatoms to cyanobacteria occurring later in the year (see section 4.2). In addition, low light extinction is prolonging the seasonal time window for *P. rubescens* and therefore allows to persist longer towards the end of the year. Similarly, since in all of the L (light extinction) scenarios, *P. rubescens* appeared in the metalimnion around the same time (i.e., around day 125), the results indicate that lower extinction extends the duration of its exponential growth phase. The L- scenarios point to the importance of light conditions for *P. rubescens* population dynamics, which is mediated by direct (as a growth-limiting resource) as well as indirect processes (by shifting resource competition within the phytoplankton community).

4. Discussion

We used a well-established water quality model (W2) to demonstrate the influence of water withdrawal strategies and light extinction on the growth of the cyanobacteria *P. rubescens* in Rappbode Reservoir, the largest drinking water reservoir in Germany. Although the occurrence (Ernst et al., 2009), physiology (Selmeczy et al., 2016) and the toxicity of *P. rubescens* (Viaggiu et al., 2004) have been well studied, little is known about active strategies to control blooms of this species. This is a major gap in current research as this highly specialized cyanophyte can proliferate in nutrient-poor water bodies, which often serve as drinking water sources. Indeed, existing research on cyanobacterial blooms focus largely on surface blooming and scum forming algae in eutrophic waters like Lake Taihu (Huang et al., 2020) or recent Lake

Erie (Pirasteh et al., 2020). But research has only superficially addressed subsurface blooms like those typically formed by *P. rubescens*. This study advances our knowledge in this respect by adding three novelties: (i) providing an ecosystem model for the prediction of subsurface blooms, (ii) generate concrete reservoir operation strategies to mitigate subsurface blooms in Germany's largest drinking water reservoir, and (iii) identify key environmental factors (light) that affect their occurrence. Needless to say, other environmental factors like nutrient supply and distribution are similarly important and require more research in future.

Note that *P. rubescens* has a low specific chlorophyll a content meaning that its biomass is not as low as suggested by the small chlorophyll values. Moreover, Rappbode is an oligotrophic water body and the formation of such a cyanobacteria population is outstanding and alerting the context of drinking water provisioning. Meanwhile, *P. rubescens* can contain high microcystin toxin quota, so only a small amount of algae can severely harm the human health and lake ecosystem. Survey data from German water bodies indicated the total microcystin content in *P. rubescens* ranges from 2000–5000 ug/g dry weight (Chorus and Welker, 2021). So the biomass of 4 ug/L (i.e. mean concentration in scenario R) corresponds to a total microcystin concentration of 1.44–3.6 ug/l, which is higher than the threshold for the drinking water sources from the WHO guideline (1 ug/l, see WHO (2004)). Considering its harmful effect on water quality, consequently, it is beneficial for the reservoir operators to suppress the growth of *P. rubescens*.

4.1. Selective water withdrawal and its influence on growth of *P. rubescens*

Selective water withdrawal is widely used in stratified reservoirs worldwide (Deng et al., 2011) for optimizing variables that collectively influence water quality (e.g., water temperature, dissolved oxygen concentration, turbidity) within the reservoir or for implementing natural downstream temperature regimes as a component of environmental flows (Olden and Naiman, 2010). Various types of infrastructure are adapted to achieve selective withdrawal, such as multi-level offtake towers, temperature-controlled curtains, floating outlets, pivoted pipes or stop-lot gates (Ren et al., 2020) and each infrastructure component has specific options and restrictions that influence its application. Outlet towers, for example, can only be used to withdraw water at specific depths while pivoted pipes can be freely moved in the vertical direction to take out water over a continuous depth range. Most previous studies of selective withdrawal have focused on temperature dynamics in the downstream river (Zheng et al., 2017; Weber et al., 2017) or within the reservoir (Mi et al., 2019; Çalışkan and Elçi, 2009). Although the same strategy is in principle also applicable for biogeochemical variables like algal biomass, nutrient concentrations and pathogens, such applications had been rarely used or modelled (Zhang et al., 2013; Feldbauer et al., 2020). Our study fills this gap and its practical value should help stakeholders optimize their management strategies and mitigate water quality problems arising from the occurrence of *P. rubescens*.

The location of peak *P. rubescens* biomass in the water column corresponds to a physiologically adjustable depth of neutral buoyancy, and may vary in different water bodies (Maltese et al., 2012) and over time due to changing light and nutrient gradients (Walsby et al., 2004). It is advantageous if the withdrawal facility can precisely follow the depth of the *P. rubescens* peak in order to maximize its potential for the algae removal. We therefore designed withdrawal depth by distance under the water surface, instead of the commonly absolute elevation. This is meaningful since the outtake depth follows the algal peak even in case of water level changes due to hypolimnetic withdrawal of raw water. Moreover, we believe that the selective withdrawal strategy, tested in this study, could remove other harmful or unwanted constituents (e.g., high concentrations of dissolved organic carbon or heavy metals) in reservoirs, as long as its occurrence is restricted to a narrow depth range and the offtake can directly flush the layer containing the constituents out of the water column (Rigosi and Rueda, 2012).

Our results also indicate that *P. rubescens* concentrations decreased following the increased water withdrawal volume, but the relative effectiveness in the algae removal per unit of water withdrawn, is getting weaker at high withdrawal discharge (see Fig. 4). For example, the decrease of *P. rubescens* concentration is much lower from scenario V_2 to V_{\max} , than from scenario V_{\min} to V_1 . This results should be attributed to the changes of stratification intensity under different withdrawal scenarios. Here the intensity is represented by buoyancy frequency (N^2) based on the density gradient in water column, which is calculated as (Read et al., 2011):

$$N^2 = \frac{g}{\rho} \frac{d\rho}{dz} \quad (3)$$

where g is the the acceleration due to gravity, ρ is density and z is depth. The results clearly show that during summer metalimnetic N^2 under scenario V_2 onwards is higher than that under the first two scenarios (V_{\min} and V_1 , see Fig. S3). This indicates high rates of withdrawal increase the stratification intensity and provide a more stable density gradient, which is beneficial to *P. rubescens* growth. Also, high withdrawal can be disadvantageous with respect to the loss of water storage. For example, from scenario V_1 to V_{\max} , the water level decreased by approximately 5 m for each 10 million m^3 of water withdrawn (Fig. 3). From a stakeholders' perspective, such a dramatic decrease in water level harms water security for drinking water supply, and could have negative influences on water quality due to increases in turbidity and nutrients (Zohary and Ostrovsky, 2011). Therefore, in most cases there should exist an optimal withdrawal volume for the specific research place (around 10 million m^3 in our case), balancing positive and negative effects.

Withdrawing metalimnetic water at the beginning of *P. rubescens* growth more effectively reduced its concentration in the reservoir than later withdrawals (see Figs. 5 & 6). On the one hand, this makes sense as withdrawal is exactly at the time when growth rate is maximal, but on the other hand the accumulated amount of exported biomass should be lower than for a period with later withdrawal. We hypothesize that

selective withdrawal – besides the direct effect of biomass export – also induces indirect effects on *P. rubescens* growth by changing the dynamics of soluble reactive phosphorus (SRP) concentration. The supply of phosphorus in the initial *P. rubescens* growth phase appeared to be partly recycled from diatom death. Our simulations indicated that diatoms took up a large proportion of the bioavailable phosphorus in spring before dying, with mineralization then recycling organic phosphorus to its bioavailable inorganic form, again. *P. rubescens* appeared to fill in a niche that exploited this recycled phosphorus. Scenarios with early withdrawal removed a substantial amount of mineralized phosphorus from the system, which was confirmed in our results: SRP concentration at depth 10–12 m, where *P. rubescens* was highest, was always lower in the T_{early} scenarios than in the case of late withdrawal or the reference simulation (up to 2 µg L⁻¹ in some cases, see Fig. S4). Since phytoplankton in Rappbode Reservoir is P-limited (Wentzky et al., 2018), the reduction in phosphorus concentration in the T_{early} scenarios leads to lower biomass of *P. rubescens* compared with the T_{bloom} and T_{late} scenarios. What's more, the T-scenarios showed that early withdrawal increases the diatom biomass in the surface layers (Fig. S5) which implies a stronger shading effect from diatoms on the *P. rubescens* residing in the metalimnion, leading to further deterioration of growth conditions for this species.

In the scenarios above, we separately checked the optimal withdrawal volume and timing to suppress the bloom of *P. rubescens*. To further clarify the conclusion, we coupled scenario V and scenario T together and established another 15 sub-scenarios (scenario VT) in which the optimal discharge (10 million m³) was evenly withdrawn at the metalimnion during 23 days (corresponding to the daily discharge of 5 m³ s⁻¹), starting from day 133 to 231 at one-week intervals. Here all the other settings are the same as before. Quite close to those from scenario T, the new results suggested that the population of *P. rubescens* was much lower under the strategy applied at its early growth stage than the other two stages (see Fig. S6), which further verified our previous conclusion and the robustness of the study (i.e. the optimal timing is independent of the withdrawal discharge).

Given its main purpose as a drinking water reservoir, the water storage in Rappbode Reservoir needs to be maintained above a certain volume for water security purposes (10 million m³ as absolute minimum according to the regulation of the reservoir authority). Since the water level decreases from spring to autumn in Rappbode Reservoir (Mi et al., 2019), the amount of water potentially available for withdrawal also decreases over the season. The selective withdrawal strategy should therefore remain within a “safe operating space” (see Fig. 8) that allows substantial control of *Planktothrix* biomass on the one hand, and guarantees adequate water storage on the other hand.

4.2. The role of light intensity in the algae growth in Rappbode Reservoir

Light intensity is a key factor influencing algal growth in aquatic systems, particularly for subsurface populations that are strongly affected by light extinction within the surface waters (Knapp et al., 2021). In the metalimnion, PAR from spring to autumn exceeded 0.5 mol m⁻² day⁻¹ and was up to 1.5 mol m⁻²

day⁻¹ under clear-water conditions (scenario L_{0.35}). In comparison, PAR ranged from 0.1 to 0.5 mol m⁻² day⁻¹ in the reference simulation ($\epsilon_b = 0.45 \text{ m}^{-1}$), and remained below 0.2 mol m⁻² day⁻¹ for $\epsilon_b \geq 0.55 \text{ m}^{-1}$ (see Fig. S7). In our algal growth model, saturating light intensities are 14 mol m⁻² day⁻¹ and 3.2 mol m⁻² day⁻¹ for diatoms and *P. rubescens*, respectively (see Mi et al., 2020a), indicating substantial light limitation, especially for diatoms, in the metalimnion. Interestingly, since diatoms undergo rapid development in spring (i.e., before the growth of *P. rubescens*) and monopolize nutrients in their biomass (Wentzky et al., 2019), scenario L_{0.35} allowed a longer metalimnetic persistence of diatoms (see Fig. S8), which in turn delayed the growth and occurrence of *P. rubescens* (see Fig. 7). Again, this points to the importance of indirect effects among phytoplankton groups and a proper representation of community dynamics and competition among algal groups is required to capture the dynamics at a species level.

Current climate forecasts indicate that due to global warming, air temperature for the study region may increase substantially in this century (Mi et al., 2020b), which will intensify stratification duration and stability potentially supporting the dominance of *P. rubescens* in lakes and reservoirs (Knapp et al., 2021). Our study suggests that decreasing light intensity in the metalimnion may offset the supportive effects of warming on the *P. rubescens* growth. A number of studies have reported increasing DOC concentrations (i.e. brownification, see Kritzberg et al. (2020)) in surface waters. This brownification, which is observable at continental scales (Monteith et al., 2007), is coming along with higher light extinction that is interfering with primary production by reducing light availability (Karlsson et al., 2009). Light conditions in the metalimnion are strongly affected by brownification and rising DOC concentrations can effectively shrink or even close the ecological niche for *P. rubescens*. Several drivers can lead to the brownification including changes in climate conditions and land cover, and reduction in atmospheric acid deposition. Faster flushing rates due to increasing precipitation, for example, restrain DOC sedimentation which leads to elevated DOC. To get a better quantitative understanding about the role of brownification for *P. rubescens* dynamics, further model applications should take these processes into account and deliver useful information for the reservoir operators.

4.3 Limitations and future work

The water quality model used in this research systematically elucidates the influence of two important driving factors (i.e., metalimnetic water withdrawal and background light conditions) on *P. rubescens* growth in Rappbode Reservoir. To extend the current study, our model can be used as a template to assess the possibility to also control other harmful algae by selective withdrawal, e.g., species associated with surface blooms. For achieving this goal, further model development may be required, e.g. to include other algal groups and new features like vertical migration of phytoplankton cells associated with buoyancy control.

Additionally, although metalimnetic water withdrawal can effectively suppress *P. rubescens* growth, the water that is withdrawn could potentially release high levels of cyanobacteria into downstream ecosystems. As indicated by Teurlincx et al. (2019), ecological functioning of inland waters can only be comprehensively understood if we take their connections with upstream catchments and downstream

receiving waters into account. Accordingly, for future studies, it is recommended to combine upstream catchment models with lake models, as well as models of downstream ecosystems, in order to upscale the research from local to regional perspective and develop system-level management strategies.

5. Conclusions

In this work, we applied a well-established water quality model (CE-QUAL-W2) to illustrate the effect of water withdrawal strategies and light extinction on the growth of the cyanobacteria *P. rubescens* in Rappbode Reservoir, Germany's largest drinking water reservoir. The results showed that the selective withdrawal strategy is an effective way to reduce the biomass of *P. rubescens* in the reservoir. Through a scenario analysis we identified the optimal withdrawal volume to suppress the *P. rubescens* bloom as 10 million m³ (around 10% of the reservoir volume) and were also able to determine an optimal seasonal time window for applying the strategy. The biomass of *P. rubescens* is most effectively suppressed when the metalimnetic withdrawal is applied at an early growth stage (i.e., day 133 to 161). Additionally, underwater light conditions were identified as an important factor for the growth of *P. rubescens* and any increase in light extinction led to lower biomass and shorter duration of the algal blooms. The algae almost disappeared when the extinction coefficient exceeded 0.55 m⁻¹. Considering the widespread occurrence of *P. rubescens* in stratified lakes and reservoirs worldwide, we believe the importance of our research extends beyond the case of Rappbode Reservoir and the results will be helpful to scientists and water managers working on strategies for other water bodies to deal with the bloom of this harmful algae.

Abbreviations

2D: two dimensional; W2: CE-QUAL-W2; *P. rubescens*: *Planktothrix rubescens*; SRP: soluble reactive phosphorus; PAR: photosynthetically active radiation

Declarations

Ethics approval and consent to participate

Not applicable

Consent for publication

Not applicable

Data availability statement

The source code of the model CE-QUAL-W2 can be freely downloaded at <http://cee.pdx.edu/w2/>. All the datasets that support the findings of this study are available from the corresponding author upon reasonable request.

Competing interests

The authors declare that they have no conflict of interest.

Funding

This project was funded within the Australia-Germany Joint Research Co-operation Scheme by the DAAD – (German Academic Exchange Service) and Universities Australia (project CYANOMOD), the newMOM-project supported by the German Science Foundation under grant DFG RI2040/4-1, the National Natural Science Foundation of China (42107060) and Xingliao Talents Plan (XLYC2002054). Xiangzhen Kong is supported by a postdoctoral fellowship from the Alexander von Humboldt Foundation in Germany. The reservoir monitoring infrastructure was financially supported by TERENO (TERrestrial ENvironmental Observatories) funded by the Helmholtz Association and the Federal Ministry of Education and Research (BMBF).

Authors' contributions

Chenxi Mi conducted the W2 modeling, with the help from David P. Hamilton and Karsten Rinke. Chenxi Mi, Marieke A. Frassl, Tom Shatwell and Karsten Rinke designed research, analyzed data and wrote the manuscript. Xiangzhen Kong, Bertram Boehrer, Yiping Li and Jan Donner reviewed, edited and proofread the manuscript. All authors read and approved the final manuscript.

Acknowledgements

We are grateful to the reservoir authority of the Rappbode Reservoir (Talsperrenbetrieb Sachsen-Anhalt) for providing data.

References

1. Abbott, M. R., Denman, K. L., Powell, T. M., Richerson, P. J., Richards, R. C., and Goldman, C. R.: Mixing and the dynamics of the deep chlorophyll maximum in Lake Tahoe 1, *Limnology and Oceanography*, 29, 862-878, 1984.
2. Abdelrhman, M. A.: Modeling Water Clarity and Light Quality in Oceans, *Journal of Marine Science and Engineering*, 4, 80, 2016.
3. Bogialli, S., Nigro di Gregorio, F., Lucentini, L., Ferretti, E., Ottaviani, M., Ungaro, N., Abis, P. P., and Cannarozzi de Grazia, M.: Management of a toxic cyanobacterium bloom (*Planktothrix rubescens*) affecting an Italian drinking water basin: a case study, *Environmental science & technology*, 47, 574-583, 2013.
4. Çalışkan, A., and Elçi, Ş.: Effects of selective withdrawal on hydrodynamics of a stratified reservoir, *Water Resour Manag*, 23, 1257-1273, 2009.
5. Carr, M. K., Sadeghian, A., Lindenschmidt, K.-E., Rinke, K., and Morales-Marin, L.: Impacts of Varying Dam Outflow Elevations on Water Temperature, Dissolved Oxygen, and Nutrient Distributions in a

- Large Prairie Reservoir, *Environ Eng Sci*, 2019.
6. Carraro, E., Guyennon, N., Hamilton, D., Valsecchi, L., Manfredi, E. C., Viviano, G., Salerno, F., Tartari, G., and Copetti, D.: Coupling high-resolution measurements to a three-dimensional lake model to assess the spatial and temporal dynamics of the cyanobacterium *Planktothrix rubescens* in a medium-sized lake, in: *Hydrobiologia*, Springer, 77-95, 2012.
 7. Chorus, I., Falconer, I. R., Salas, H. J., and Bartram, J.: Health risks caused by freshwater cyanobacteria in recreational waters, *Journal of Toxicology and Environmental Health Part B: Critical Reviews*, 3, 323-347, 2000.
 8. Chorus, I., and Welker, M.: *Toxic cyanobacteria in water: a guide to their public health consequences, monitoring and management*, Taylor & Francis, 2021.
 9. Cullen, J. J.: *Subsurface chlorophyll maximum layers: enduring enigma or mystery solved?*, 2015.
 10. D'Alelio, D., Gandolfi, A., Boscaini, A., Flaim, G., Tolotti, M., and Salmaso, N.: *Planktothrix* populations in subalpine lakes: selection for strains with strong gas vesicles as a function of lake depth, morphometry and circulation, *Freshwater Biology*, 56, 1481-1493, 2011.
 11. Dehbalaei, F. N., and Javan, M.: Assessment of Selective Withdrawal and Inflow Control on the Hydrodynamics and Water Quality of Ilam Reservoir, *Water Environ Res*, 90, 307-321, 10.2175/106143017x15131012152834, 2018.
 12. Deng, Y., Tuo, Y., Li, J., Li, K., and Li, R.: Spatial-temporal effects of temperature control device of stoplog intake for Jinping I hydropower station, *Science China Technological Sciences*, 54, 83-88, 2011.
 13. Ernst, B., Hoeger, S. J., O'Brien, E., and Dietrich, D. R.: Abundance and toxicity of *Planktothrix rubescens* in the pre-alpine Lake Ammersee, Germany, *Harmful Algae*, 8, 329-342, 2009.
 14. Fee, E. J.: The vertical and seasonal distribution of chlorophyll in lakes of the Experimental Lakes Area, northwestern Ontario: Implications for primary production estimates, *Limnology and Oceanography*, 21, 767-783, 1976.
 15. Feldbauer, J., Kneis, D., Hegewald, T., Berendonk, T. U., and Petzoldt, T.: Managing climate change in drinking water reservoirs: potentials and limitations of dynamic withdrawal strategies, *Environmental Sciences Europe*, 32, 48, 10.1186/s12302-020-00324-7, 2020.
 16. Gallina, N., Beniston, M., and Jacquet, S.: Estimating future cyanobacterial occurrence and importance in lakes: a case study with *Planktothrix rubescens* in Lake Geneva, *Aquatic Sciences*, 79, 249-263, 10.1007/s00027-016-0494-z, 2017.
 17. Gu, P., Zhang, G., Luo, X., Xu, L., Zhang, W., Li, Q., Sun, Y., and Zheng, Z.: Effects of different fluid fields on the formation of cyanobacterial blooms, *Chemosphere*, 131219, 2021.
 18. Hamilton, D. P., O'Brien, K. R., Burford, M. A., Brookes, J. D., and McBride, C. G.: Vertical distributions of chlorophyll in deep, warm monomictic lakes, *Aquatic Sciences*, 72, 295-307, 2010.
 19. Ho, J. C., Michalak, A. M., and Pahlevan, N.: Widespread global increase in intense lake phytoplankton blooms since the 1980s, *Nature*, 574, 667-670, 2019.

20. Huang, J., Zhang, Y., Arhonditsis, G. B., Gao, J., Chen, Q., and Peng, J.: The magnitude and drivers of harmful algal blooms in China's lakes and reservoirs: A national-scale characterization, *Water Research*, 181, 115902, 2020.
21. Huisman, J., Codd, G. A., Paerl, H. W., Ibelings, B. W., Verspagen, J. M. H., and Visser, P. M.: Cyanobacterial blooms, *Nature Reviews Microbiology*, 16, 471-483, 10.1038/s41579-018-0040-1, 2018.
22. Jin, J., Wells, S. A., Liu, D., Yang, G., Zhu, S., Ma, J., and Yang, Z.: Effects of water level fluctuation on thermal stratification in a typical tributary bay of Three Gorges Reservoir, China, *PeerJ*, 7, e6925, <http://dx.doi.org/10.7717/peerj.6925>, 2019.
23. Karlsson, J., Byström, P., Ask, J., Ask, P., Persson, L., and Jansson, M.: Light limitation of nutrient-poor lake ecosystems, *Nature*, 460, 506-509, 2009.
24. Kirk, J. T.: *Light and photosynthesis in aquatic ecosystems*, Cambridge university press, 1994.
25. Knapp, D., Fernández Castro, B., Marty, D., Loher, E., Köster, O., Wüest, A., and Posch, T.: The Red Harmful Plague in Times of Climate Change: Blooms of the Cyanobacterium *Planktothrix rubescens* Triggered by Stratification Dynamics and Irradiance, *Front. Microbiol.*, 12, 10.3389/fmicb.2021.705914, 2021.
26. Kobler, U. G., Wüest, A., and Schmid, M.: Effects of Lake-Reservoir Pumped-Storage Operations on Temperature and Water Quality, *Sustainability*, 10, 1968, <https://doi.org/10.3390/su10061968>, 2018.
27. Kong, X., Seewald, M., Dadi, T., Friese, K., Mi, C., Boehrer, B., Schultze, M., Rinke, K., and Shatwell, T.: Unravelling winter diatom blooms in temperate lakes using high frequency data and ecological modeling, *Water Research*, 190, 116681, 2021.
28. Kritzberg, E. S., Hasselquist, E. M., Škerlep, M., Löfgren, S., Olsson, O., Stadmark, J., Valinia, S., Hansson, L.-A., and Laudon, H.: Browning of freshwaters: Consequences to ecosystem services, underlying drivers, and potential mitigation measures, *Ambio*, 49, 375-390, 10.1007/s13280-019-01227-5, 2020.
29. Kurmayer, R., and Gumpenberger, M.: Diversity of microcystin genotypes among populations of the filamentous cyanobacteria *Planktothrix rubescens* and *Planktothrix agardhii*, *Mol Ecol*, 15, 3849-3861, 2006.
30. Leach, T. H., Beisner, B. E., Carey, C. C., Pernica, P., Rose, K. C., Huot, Y., Brentrup, J. A., Domaizon, I., Grossart, H. P., and Ibelings, B. W.: Patterns and drivers of deep chlorophyll maxima structure in 100 lakes: The relative importance of light and thermal stratification, *Limnology and Oceanography*, 63, 628-646, 2018.
31. Lewis Jr, W. M., Wurtsbaugh, W. A., and Paerl, H. W.: Rationale for control of anthropogenic nitrogen and phosphorus to reduce eutrophication of inland waters, *Environmental science & technology*, 45, 10300-10305, 2011.
32. Lüring, M., Mucci, M., and Waajen, G.: Removal of Positively Buoyant *Planktothrix rubescens* in Lake Restoration, *Toxins (Basel)*, 12, 700, 2020.

33. Maltese, A., Capodici, F., Ciraolo, G., La Loggia, G., Granata, A., and Corbari, C.: Planktothrix rubescens in freshwater reservoirs: remote sensing potentiality for mapping cell density, *Remote Sensing for Agriculture, Ecosystems, and Hydrology XIV*, 2012, 85311X,
34. Mi, C., Sadeghian, A., Lindenschmidt, K.-E., and Rinke, K.: Variable withdrawal elevations as a management tool to counter the effects of climate warming in Germany's largest drinking water reservoir, *Environmental Sciences Europe*, 31, 19, 2019.
35. Mi, C., Shatwell, T., Ma, J., Wentzky, V. C., Boehrer, B., Xu, Y., and Rinke, K.: The formation of a metalimnetic oxygen minimum exemplifies how ecosystem dynamics shape biogeochemical processes: A modelling study, *Water Research*, <https://doi.org/10.1016/j.watres.2020.115701>, 2020a.
36. Mi, C., Shatwell, T., Ma, J., Xu, Y., Su, F., and Rinke, K.: Ensemble warming projections in Germany's largest drinking water reservoir and potential adaptation strategies, *Science of The Total Environment*, 141366, <https://doi.org/10.1016/j.scitotenv.2020.141366>, 2020b.
37. Mishra, S., Stumpf, R. P., Schaeffer, B. A., Werdell, P. J., Loftin, K. A., and Meredith, A.: Measurement of Cyanobacterial Bloom Magnitude using Satellite Remote Sensing, *Sci. Rep.*, 9, 18310, [10.1038/s41598-019-54453-y](https://doi.org/10.1038/s41598-019-54453-y), 2019.
38. Monteith, D. T., Stoddard, J. L., Evans, C. D., de Wit, H. A., Forsius, M., Høgåsen, T., Wilander, A., Skjelkvåle, B. L., Jeffries, D. S., Vuorenmaa, J., Keller, B., Kopáček, J., and Vesely, J.: Dissolved organic carbon trends resulting from changes in atmospheric deposition chemistry, *Nature*, 450, 537-540, [10.1038/nature06316](https://doi.org/10.1038/nature06316), 2007.
39. Muggeo, V. M., and Muggeo, M. V. M.: Package 'segmented', *Biometrika*, 58, 516, 2017.
40. Olden, J. D., and Naiman, R. J.: Incorporating thermal regimes into environmental flows assessments: modifying dam operations to restore freshwater ecosystem integrity, *Freshwater Biology*, 55, 86-107, 2010.
41. Padisák, J., Crossetti, L. O., and Naselli-Flores, L.: Use and misuse in the application of the phytoplankton functional classification: a critical review with updates, *Hydrobiologia*, 621, 1-19, 2009.
42. Paerl, H. W.: Mitigating toxic planktonic cyanobacterial blooms in aquatic ecosystems facing increasing anthropogenic and climatic pressures, *Toxins (Basel)*, 10, 76, 2018.
43. Park, H., Chung, S., Cho, E., and Lim, K.: Impact of climate change on the persistent turbidity issue of a large dam reservoir in the temperate monsoon region, *Climatic Change*, 1-14, <http://dx.doi.org/10.1007/s10584-018-2322-z>, 2018.
44. Pirasteh, S., Mollaee, S., Fatholahi, S. N., and Li, J.: Estimation of Phytoplankton Chlorophyll-a Concentrations in the Western Basin of Lake Erie Using Sentinel-2 and Sentinel-3 Data, *CaJRS*, 46, 585-602, 2020.
45. Posch, T., Koster, O., Salcher, M. M., and Pernthaler, J.: Harmful filamentous cyanobacteria favoured by reduced water turnover with lake warming, *Nature Climate Change*, 2, 809-813, <https://dx.doi.org/10.1038/nclimate1581>, 2012.

46. Rastogi, R. P., Madamwar, D., and Incharoensakdi, A.: Bloom Dynamics of Cyanobacteria and Their Toxins: Environmental Health Impacts and Mitigation Strategies, *Front. Microbiol.*, 6, 10.3389/fmicb.2015.01254, 2015.
47. Read, J. S., Hamilton, D. P., Jones, I. D., Muraoka, K., Winslow, L. A., Kroiss, R., Wu, C. H., and Gaiser, E.: Derivation of lake mixing and stratification indices from high-resolution lake buoy data, *Environmental Modelling and Software*, 26, 1325-1336, <http://dx.doi.org/10.1016/j.envsoft.2011.05.006>, 2011.
48. Ren, W., Wei, J., Xie, Q., Miao, B., and Wang, L.: Experimental and Numerical Investigations of Hydraulics in Water Intake with Stop-Log Gate, *Water*, 12, 1788, 2020.
49. Reynolds, C. S.: *The ecology of phytoplankton*, Cambridge University Press, 2006.
50. Rigosi, A., and Rueda, F. J.: Hydraulic control of short-term successional changes in the phytoplankton assemblage in stratified reservoirs, *Ecol Eng*, 44, 216-226, <https://doi.org/10.1016/j.ecoleng.2012.04.012>, 2012.
51. Rinke, K., Kuehn, B., Bocaniov, S., Wendt-Potthoff, K., Buttner, O., Tittel, J., Schultze, M., Herzsprung, P., Ronicke, H., Rink, K., Rinke, K., Dietze, M., Matthes, M., Paul, L., and Friese, K.: Reservoirs as sentinels of catchments: the Rappbode Reservoir Observatory (Harz Mountains, Germany), *Environmental Earth Sciences*, 69, 523-536, <http://dx.doi.org/10.1007/s12665-013-2464-2>, 2013.
52. Selmečzy, G. B., Tapolczai, K., Casper, P., Krienitz, L., and Padisák, J.: Spatial-and niche segregation of DCM-forming cyanobacteria in Lake Stechlin (Germany), *Hydrobiologia*, 764, 229-240, 2016.
53. Shatwell, T., Thiery, W., and Kirillin, G.: Future projections of temperature and mixing regime of European temperate lakes, *Hydrology and Earth System Sciences*, 23, 1533-1551, 2019.
54. Teurlincx, S., van Wijk, D., Mooij, W. M., Kuiper, J. J., Huttunen, I., Brederveld, R. J., Chang, M., Janse, J. H., Woodward, B., and Hu, F.: A perspective on water quality in connected systems: modelling feedback between upstream and downstream transport and local ecological processes, *Current Opinion in Environmental Sustainability*, 40, 21-29, 2019.
55. Trbojević, I., Blagojević, A., Kostić, D., Marjanović, P., Krizmanić, J., Popović, S., and Simić, G. S.: Periphyton development during summer stratification in the presence of a metalimnetic bloom of *Planktothrix rubescens*, *Limnologica*, 78, 125709, 2019.
56. Viaggiu, E., Melchiorre, S., Volpi, F., Di Corcia, A., Mancini, R., Garibaldi, L., Crichigno, G., and Bruno, M.: Anatoxin-a toxin in the cyanobacterium *Planktothrix rubescens* from a fishing pond in northern Italy, *Environmental Toxicology: An International Journal*, 19, 191-197, 2004.
57. Walsby, A., AE, W., and HC, U.: Buoyancy changes of a red coloured *Oscillatoria agardhii* in Lake Gjersjoen, Norway, 1983.
58. Walsby, A., and Schanz, F.: Light-dependent growth rate determines changes in the population of *Planktothrix rubescens* over the annual cycle in Lake Zürich, Switzerland, *New Phytol*, 154, 671-687, 2002.
59. Walsby, A. E., Ng, G., Dunn, C., and Davis, P. A.: Comparison of the depth where *Planktothrix rubescens* stratifies and the depth where the daily insolation supports its neutral buoyancy, *New*

- Phytol, 162, 133-145, 2004.
60. Walsby, A. E., and Jüttner, F.: The uptake of amino acids by the cyanobacterium *Planktothrix rubescens* is stimulated by light at low irradiances, *Fems Microbiol Ecol*, 58, 14-22, 2006.
 61. Weber, M., Rinke, K., Hipsey, M., and Boehrer, B.: Optimizing withdrawal from drinking water reservoirs to reduce downstream temperature pollution and reservoir hypoxia, *Journal of Environmental Management*, 197, 96-105, 2017.
 62. Wentzky, V. C., Tittel, J., Jäger, C. G., and Rinke, K.: Mechanisms preventing a decrease in phytoplankton biomass after phosphorus reductions in a German drinking water reservoir—results from more than 50 years of observation, *Freshwater biology*, 63, 1063-1076, <http://dx.doi.org/10.1111/fwb.13116>, 2018.
 63. Wentzky, V. C., Frassl, M. A., Rinke, K., and Boehrer, B.: Metalimnetic oxygen minimum and the presence of *Planktothrix rubescens* in a low-nutrient drinking water reservoir, *Water Research*, 208-218, 2019.
 64. WHO: Back ground document or development of WHO Guidelines for drinking-water quality, Fax, 41, 791, 2004.
 65. Williams, D. T.: Determination of light extinction coefficients in lakes and reservoirs, *Proceeding of the Symposium on Surface Water Impoundments*, American Society of Civil Engineers, 1981, 1329-1335,
 66. Williams, G. N., Larouche, P., Dogliotti, A. I., and Latorre, M. P.: Light Absorption by Phytoplankton, Non-Algal Particles, and Dissolved Organic Matter in San Jorge Gulf in Summer, *Oceanography*, 31, 40-49, 2018.
 67. Zhang, M., Lin, Q.-Q., Xiao, L.-J., Wang, S., Qian, X., and Han, B.-P.: Effect of intensive epilimnetic withdrawal on phytoplankton community in a (sub) tropical deep reservoir, *J. Limnol.*, 72, e35-e35, 2013.
 68. Zheng, T., Sun, S., Liu, H., Xia, Q., and Zong, Q.: Optimal control of reservoir release temperature through selective withdrawal intake at hydropower dam, *Water Science and Technology: Water Supply*, 17, 279-299, 2017.
 69. Zhou, Y., Davidson, T. A., Yao, X., Zhang, Y., Jeppesen, E., de Souza, J. G., Wu, H., Shi, K., and Qin, B.: How autochthonous dissolved organic matter responds to eutrophication and climate warming: evidence from a cross-continental data analysis and experiments, *Earth-sci Rev*, 185, 928-937, 2018.
 70. Zohary, T., and Ostrovsky, I.: Ecological impacts of excessive water level fluctuations in stratified freshwater lakes, *Inland Waters*, 1, 47-59, 2011.

Figures



Figure 1

Map of Germany (top left). The black point indicates the location of Rappbode Reservoir. Bathymetric map of the Rappbode Reservoir (right). The black point shows the sampling location. The red number shows the location of three pre-reservoirs: \boxtimes Rappbode, \boxtimes Hassel, \boxtimes Koenigshuette.

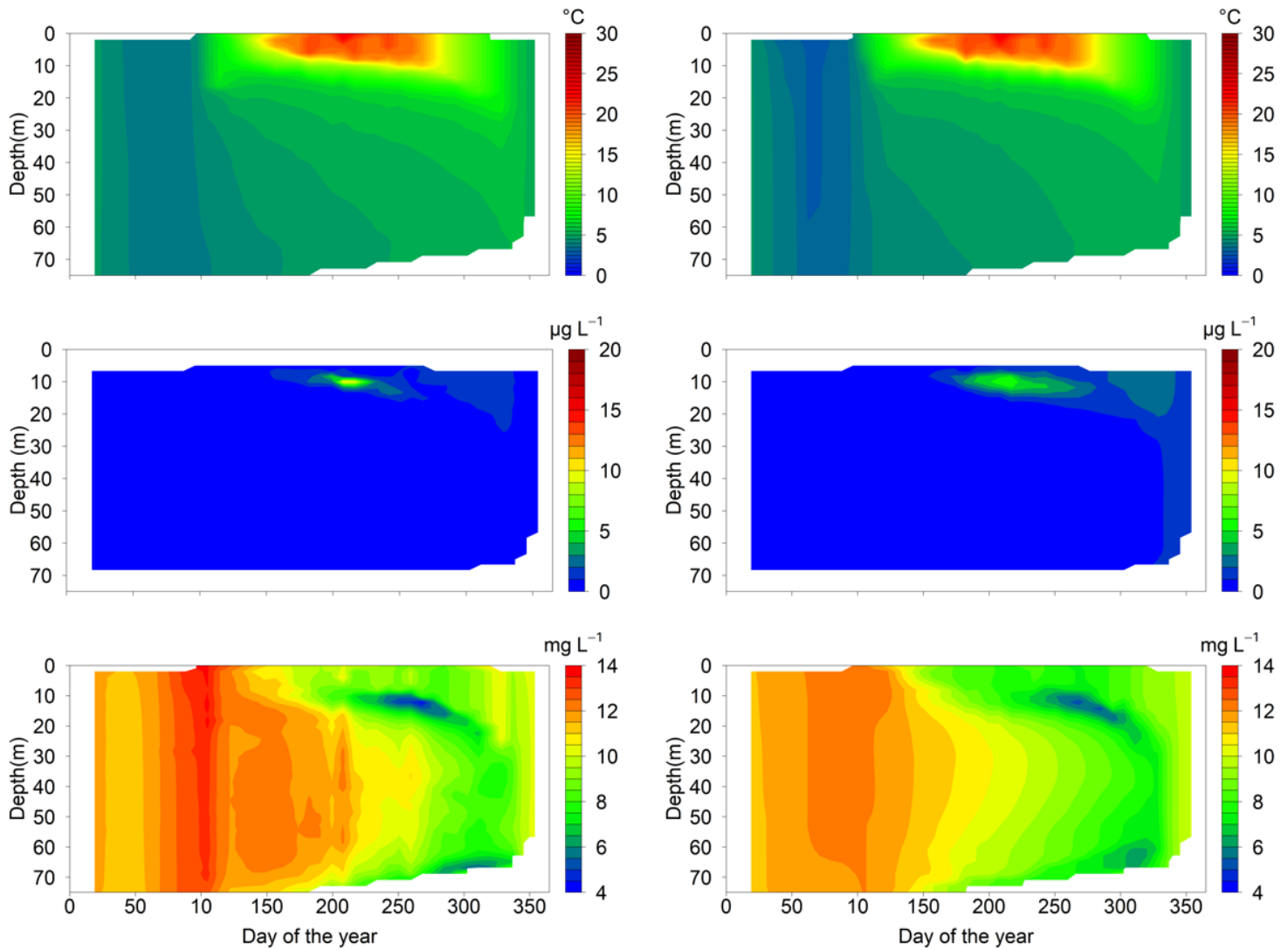


Figure 2

Observed (left) and simulated (right) results for: water temperature (top), *P. rubescens* concentration (in terms of chlorophyll *a*, middle) and oxygen concentration (bottom) in 2016 in Rappbode Reservoir.

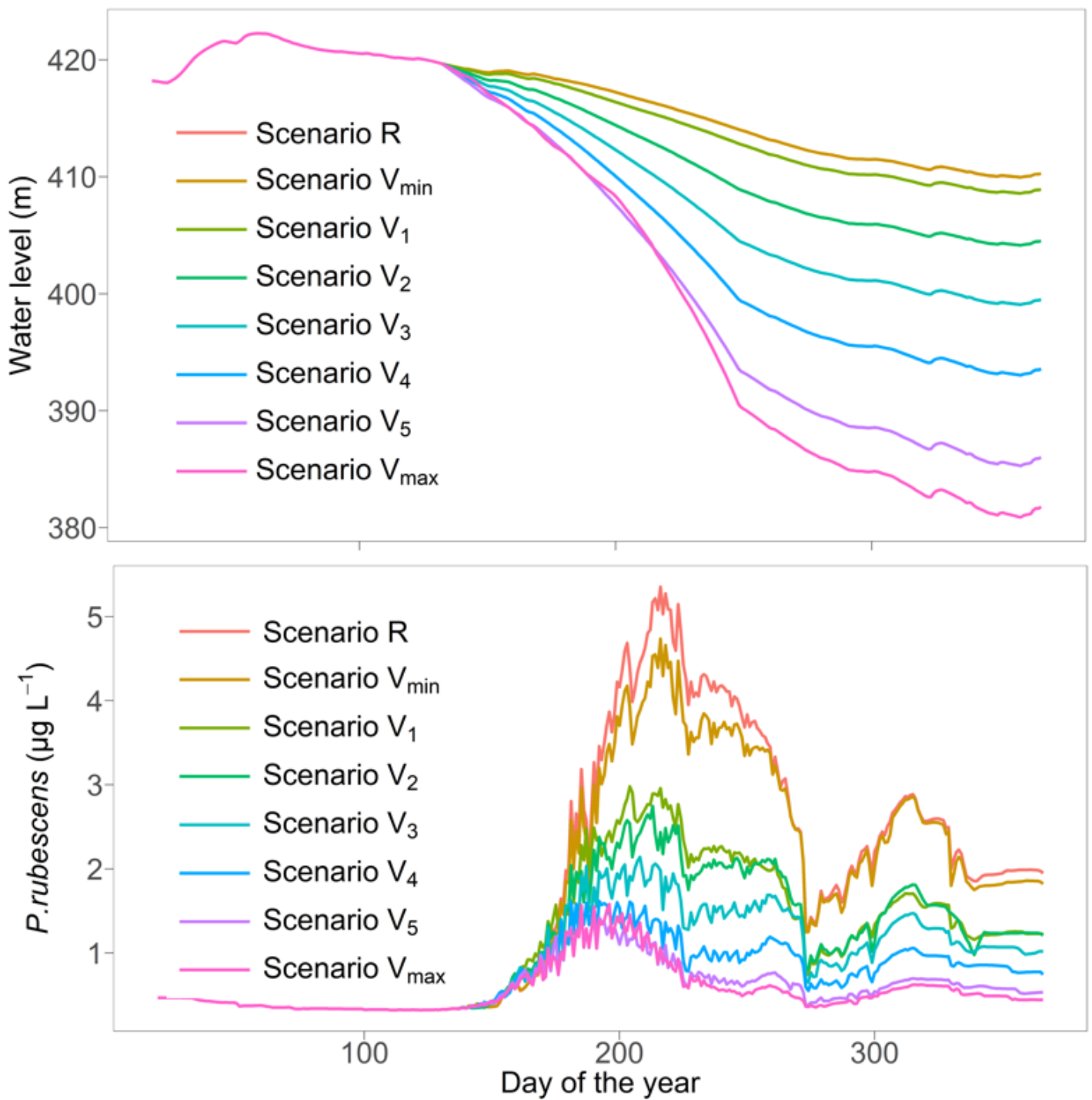


Figure 3

Water level (top) and concentration of *P. rubescens* (bottom, as chlorophyll *a*) in the metalimnion (i.e., between 10 - 12 m) under scenarios R and V (see Table 1 for details). Note that in the upper plots, the lines for R and V_{min} are plotted on top of each other.

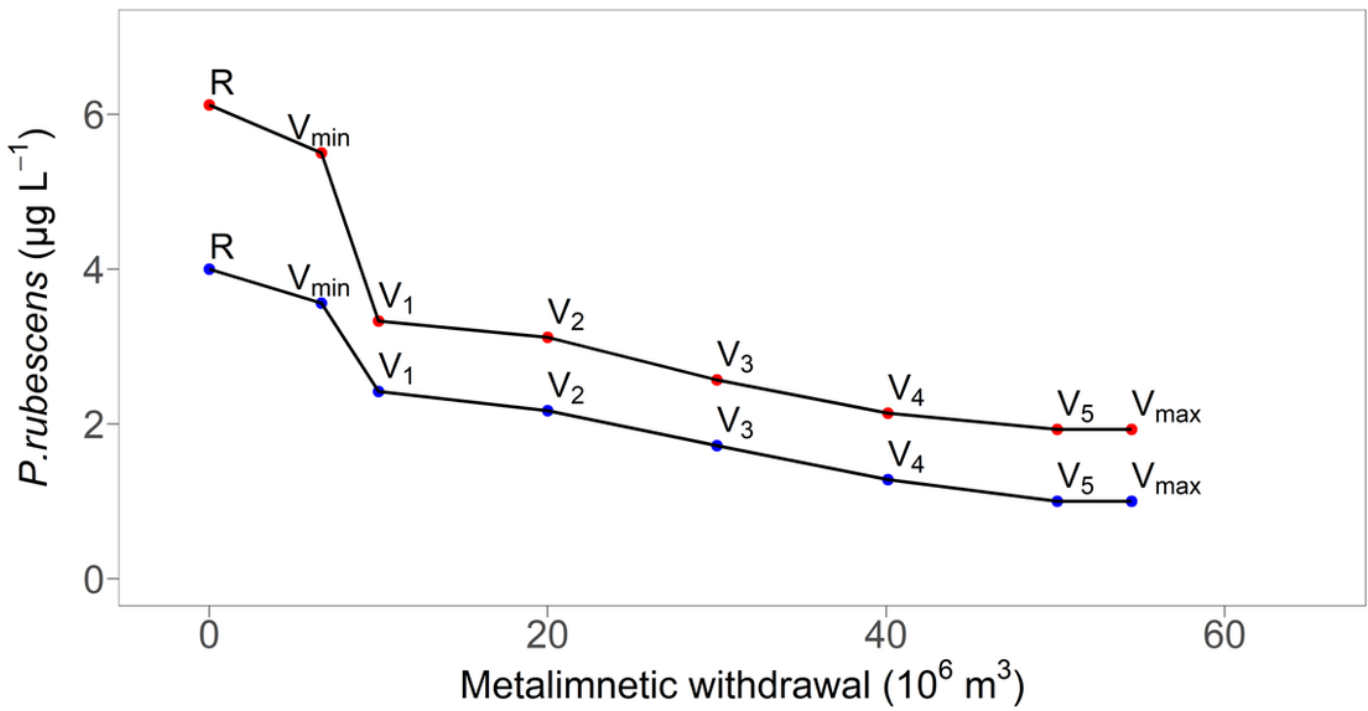


Figure 4

Average (blue points) and the maximum (red points) concentration of *P. rubescens* (as chlorophyll *a*) in the metalimnion during summer (between 10 and 12 m, from day 180 to 240) under scenario R and V (see Table 1 for details).

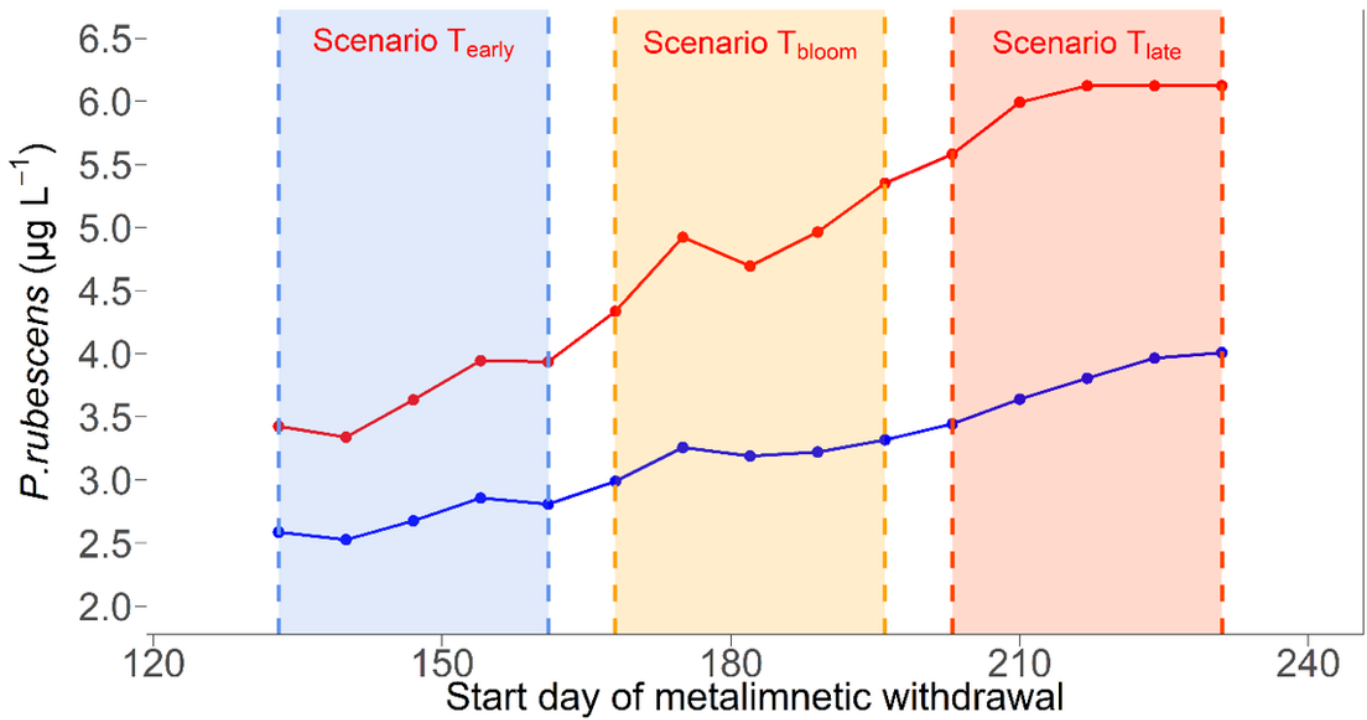


Figure 5

Average (blue line) and the maximum (red line) *P. rubescens* concentration (as chlorophyll *a*) in the metalimnion during summer (10 to 12 m, from day 180 to 240) under scenario T (see Table 1 for details). The shades show different periods of *P. rubescens* growth used in subsequent scenarios

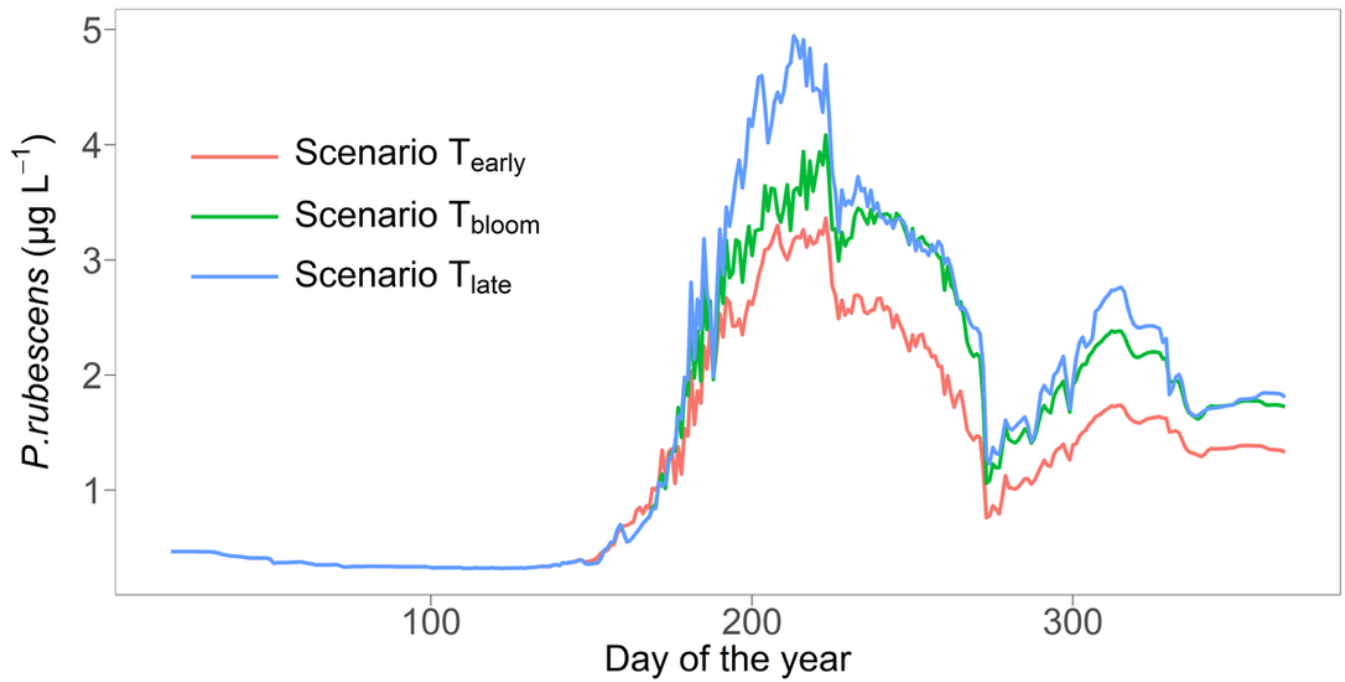


Figure 6

Concentration of *P. rubescens* (as chlorophyll *a*) in the metalimnion (10 to 12 m) for 2016 under scenario T. Each line indicates the mean result from 5 sub-scenarios included.

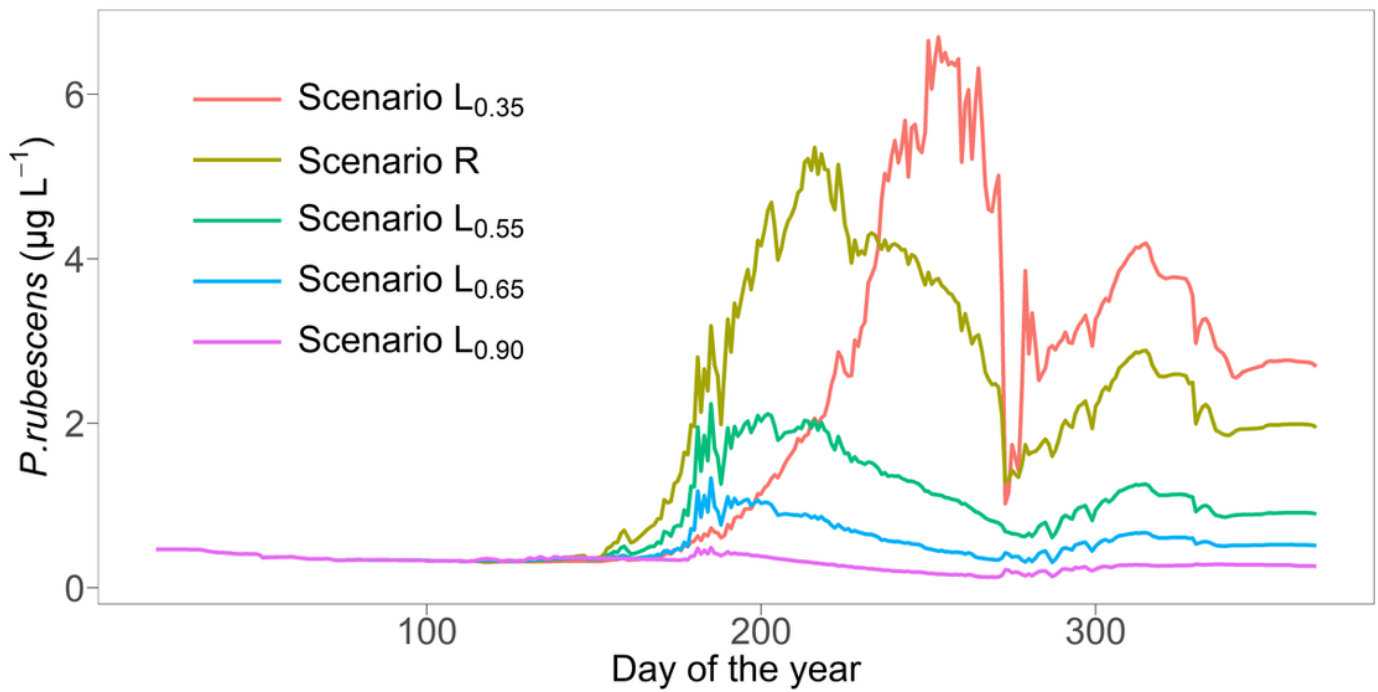


Figure 7

Concentration of *P. rubescens* (as chlorophyll *a*) in the metalimnion (10 to 12 m) under scenario R and L (see Table 1 for details).

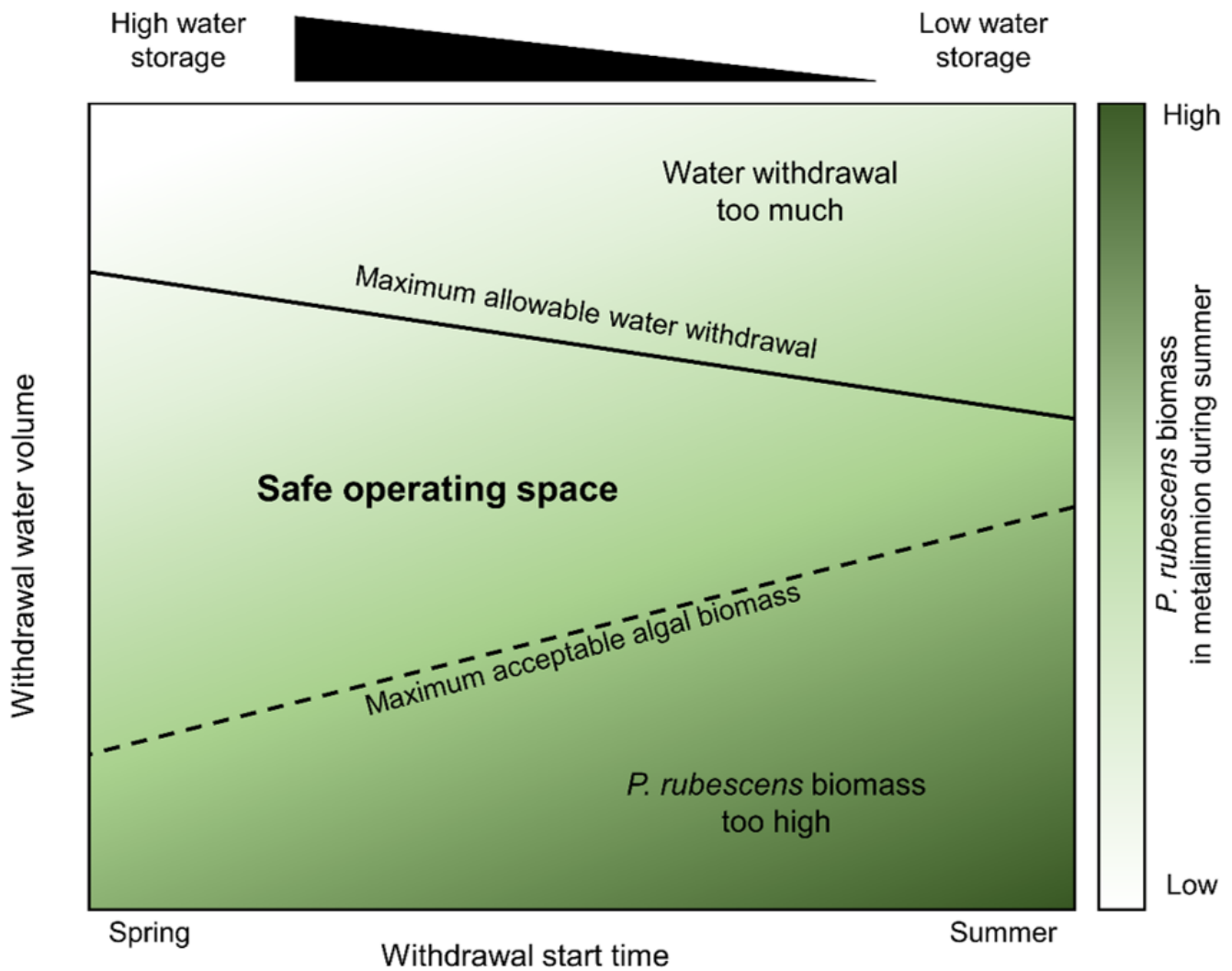


Figure 8

A conceptual diagram showing the pattern of maximum biomass of *P. rubescens* in the metalimnion of Rappbode Reservoir in summer, under different combinations of withdrawal water volume and withdrawal start time. The pattern is generated from the scenario analysis, which indicates that the phytoplankton biomass would be lower with higher withdrawal volumes and earlier withdrawal (given as color scale, i.e., decreasing towards the upper left corner). The solid line is the maximum withdrawal water volume that allows adequate water storage in the reservoir. The maximum allowable water withdrawal decreases over the season because the stored water volume declines from spring to summer. The phytoplankton biomass threshold (dashed line) is a critical upper level of *P. rubescens* that can

prevent the subsequent development of high concentrations. It increases over the season since earlier metalimnetic withdrawal can more effectively suppress the algae growth compared to the later withdrawal. Between the two lines is the safe operating space as a tradeoff between mitigating harmful algal blooms and maintaining water resources.

Supplementary Files

This is a list of supplementary files associated with this preprint. Click to download.

- [Supplementalmaterial.docx](#)